

Fluid-Phase Markers in the Basolateral Endocytic Pathway Accumulate in Response to the Actin Assembly-promoting Drug Jasplakinolide

Wenda Shurety, Nancy L. Stewart, and Jennifer L. Stow*

Centre for Molecular and Cellular Biology, University of Queensland, Brisbane, Queensland 4072, Australia

Submitted September 9, 1997; Accepted January 20, 1998
Monitoring Editor: David Drubin

To investigate the role of filamentous actin in the endocytic pathway, we used the cell-permeant drug Jasplakinolide (JAS) to polymerize actin in intact polarized Madin-Darby canine kidney (MDCK) cells. The uptake and accumulation of the fluid-phase markers fluorescein isothiocyanate (FITC)-dextran and horseradish peroxidase (HRP) were followed in JAS-treated or untreated cells with confocal fluorescence microscopy, biochemical assays, and electron microscopy. Pretreatment with JAS increased the uptake and accumulation of fluid-phase markers in MDCK cells. JAS increased endocytosis in a polarized manner, with a marked effect on fluid-phase uptake from the basolateral surface but not from the apical surface of polarized MDCK cells. The early uptake of FITC-dextran and HRP was increased more than twofold in JAS-treated cells. At later times, FITC-dextran and HRP accumulated in clustered endosomes in the basal and middle regions of JAS-treated cells. The large accumulated endosomes were similar to late endosomes but they were not colabeled for other late endosome markers, such as rab7 or mannose-6-phosphate receptor. JAS altered transport in the endocytic pathway at a later stage than the microtubule-dependent step affected by nocodazole. JAS also had a notable effect on cell morphology, inducing membrane bunching at the apical pole of MDCK cells. Although other studies have implicated actin in endocytosis at the apical cell surface, our results provide novel evidence that filamentous actin is also involved in the endocytosis of fluid-phase markers from the basolateral membrane of polarized cells.

INTRODUCTION

The actin cytoskeleton has many important roles in cellular activities such as motility, adhesion, division, stabilization of microvilli, formation of ruffles, and endocytosis. The highly ordered architecture of the actin cytoskeleton is regulated by several kinds of actin-binding proteins including cross-linking proteins, severing proteins, end-capping proteins, and monomer-sequestering proteins (Stossel *et al.*, 1985; Kreis and Vale, 1993). The regulated actions of these proteins result in the dynamic assembly and disassembly of monomeric actin into filamentous (F-) actin throughout the cell.

Previous studies have implicated the actin cytoskeleton in various endocytic membrane trafficking pathways in yeast and mammalian cells. Temperature-sensitive mutations of the yeast actin and actin-binding protein genes inhibit endocytic internalization and serve to demonstrate that the early stages of endocytosis require actin polymerization and depolymerization (Kubler and Riezman, 1993; Reizman, 1993). The use of drugs that disrupt or inhibit actin polymerization, such as cytochalasin D, have provided much of the evidence to date for actin filament involvement in processes such as endocytosis. Cytochalasins act by decreasing the rate of addition of monomeric actin molecules to the barbed fast-growing ends of actin filaments (MacLean-Fletcher and Pollard, 1980), thus inducing depolymerization of F-actin. Cytochalasin D treatment affects endocytosis in a variety

* Corresponding author.

of mammalian cells, often inducing blocks in early stages of endocytic uptake (Sandvig and van Deurs, 1990; Gottlieb *et al.*, 1993; Jackman *et al.*, 1994; Durrbach *et al.*, 1996b; Shurety *et al.*, 1996). Later stages of endocytosis, such as late-endosome/lysosome fusion (van Deurs *et al.*, 1995) and delivery of ligands to degradative compartments (Durrbach *et al.*, 1996b), have also been shown to involve actin filaments. In similar ways, the actin cytoskeleton has also been implicated in various stages of exocytosis or secretion. The cortical actin web has been shown to create a barrier preventing exocytosis of zymogen granules in pancreatic acinar cells (Muallem *et al.*, 1995). Similarly, movement of water channels to the cell surface of kidney epithelial cells involves active interaction of vesicles with the cortical actin network (Hays *et al.*, 1987). Disruption of actin polymerization thus has wide-reaching effects on trafficking throughout cells.

It is not yet clear how actin associates with, or regulates the movement, shape, or function of endocytic compartments. Staining of F-actin shows that there are actin filaments closely associated with endosomes, lysosomes, and endocytic invaginations of the cell surface (Kubler and Riezman, 1993; Durrbach *et al.*, 1996b; Murphy *et al.*, 1996). Actin-binding proteins have the potential to link organelle membranes directly with the actin cytoskeleton, and there are now several examples of such proteins associated with endocytic compartments. Myosin I, which binds both to membranes and to actin, and myosin II have been found on vesicles in endocytic and secretory pathways of mammalian cells (Fath and Burgess, 1993; Durrbach *et al.*, 1996a; Ikonen *et al.*, 1997). Deletion of the type 1 myosin genes *MYO3* and *MYO5* in yeast abolishes growth as a result of a specific defect in early steps of receptor-mediated endocytosis (Geli and Riezman, 1996). Members of the actin-binding monomeric G protein families, Rac, Rho, and Cdc42, are associated with vesicle membranes, and several different lines of evidence point to essential functional roles for these G proteins in actin filament assembly associated with endocytosis (Lamaze *et al.*, 1996; Murphy *et al.*, 1996; Ridley, 1996). Studies to date suggest that actin-binding proteins and actin filaments associate with endocytic compartments to regulate specific steps of endocytosis and also to couple endocytic trafficking to other membrane movements and cellular activities.

The surface of polarized epithelial cells is separated into apical and basolateral domains with distinct compositions of protein and lipid (Rodriguez-Boulant and Nelson, 1989). At the apical domain of polarized cells, the actin cytoskeleton is divided into two specialized domains consisting of the microvilli and the underlying terminal web, and at the basolateral domain of cultured epithelial cells, actin filaments are present as arrays of stress fibers (Brown and Stow, 1996). Endocytosis in epithelial cells occurs at both the apical and

basolateral domains. Ligands or solutes are first delivered to domain-specific early endosomes and then either transferred to late endosomes, which may be common to both the apical and basolateral endocytic pathways (Parton *et al.*, 1989; Bomsel *et al.*, 1990), or delivered to early recycling compartments, where ligands can be recycled to their respective surface or transcytosed across the cell. Previous studies using cytochalasin D have shown a domain-specific effect on endocytosis, by demonstrating that F-actin must be maintained for endocytosis of membrane markers at the apical domain of polarized epithelial cells (Gottlieb *et al.*, 1993; Jackman *et al.*, 1994).

In the present study, we used a novel approach to investigate the role of F-actin in the endocytosis of fluid-phase markers, by inducing actin polymerization in intact polarized epithelial cells. Previously, only phalloidin and a limited number of related toxins were available as agents to stabilize actin filaments; however, cells are generally impermeant to these agents (Wehland *et al.*, 1980; Joos and Gicquand, 1987). Jasplakinolide (JAS) is a cell-permeable monocyclic peptide isolated from the sea sponge *Jaspis johnstoni* (Crews *et al.*, 1986; Zabriskie *et al.*, 1986). In vitro experiments have demonstrated that JAS is a potent inducer of actin polymerization and has a much greater effect on Mg^{2+} -actin than on Ca^{2+} -actin (Bubb *et al.*, 1994). It binds to the same sites on F-actin as phalloidin and competes with it for binding (Bubb *et al.*, 1994; Senderowicz *et al.*, 1995). JAS disrupts the actin cytoskeleton in intact cells and shows potential as an antiproliferative drug in tumorigenic cells (Senderowicz *et al.*, 1995). Manipulation of intracellular actin with JAS offers the potential to study the effects of newly polymerized actin filaments and/or stabilized existing actin filaments on intracellular membrane trafficking pathways. We used JAS to study the role of F-actin in endocytosis in both polarized and nonpolarized Madin-Darby canine kidney (MDCK) cells. Our studies show that F-actin has a role in the basolateral uptake and accumulation of fluid-phase markers and in the organization of endocytic compartments.

MATERIALS AND METHODS

Cell Culture

MDCK cells, strain II, were grown as previously described in DMEM with 10% fetal calf serum and 2 mM glutamine in 5% $CO_2/95\%$ air (de Almeida and Stow, 1991; Narula *et al.*, 1992). Cells were passaged in flasks and were plated on glass coverslips or on semipermeable polycarbonate filters (Transwell; Corning Costar, Cambridge, MA) for experiments.

Immunofluorescence Staining

MDCK cells, plated at either high or low density, were grown for 3 to 4 d on coverslips or semipermeable filters. Cells were fixed in 4% paraformaldehyde and then permeabilized for 5 min in phosphate-

buffered saline (PBS) containing 0.1% Triton X-100. Fixed cells were incubated with primary antibodies followed by fluorescein isothiocyanate (FITC) or indocarbocyanine (Cy3)-conjugated secondary antibodies or probes, using bovine serum albumin in blocking/washing buffers. F-actin was labeled by incubating fixed permeabilized cells with 0.4 $\mu\text{g/ml}$ FITC-conjugated phalloidin. Coverslips or filters were mounted on glass slides in a solution of 50% glycerol/1% *n*-propyl gallate in PBS and then examined with an Olympus microscope fitted for epifluorescence. In some experiments, cells were pretreated with 1 μM JAS (Molecular Probes, Eugene, OR; diluted from a stock of 1 mM in methanol) for 45 min before processing.

FITC-Dextran Uptake

MDCK cells were grown to semiconfluence on coverslips or confluence on semipermeable filters for 3 to 4 d. Cells were washed with DMEM+ (serum-free DMEM with 10 mM HEPES, pH 7.4, 0.05% bovine serum albumin) and then incubated with or without 1 μM JAS for 45 min at 37°C. This condition for JAS preincubation was used in all experiments. For some experiments, cells were incubated with 3 μM nocodazole for 90 min prior to and during uptake. To measure fluid-phase uptake, cells were incubated for various times in DMEM+ containing 1 mg/ml FITC-dextran, (lysine-fixable anionic fluorescein-conjugated dextran, $M_r = 10,000$; Molecular Probes) in the presence or absence of 1 μM JAS. To measure uptake from apical and basolateral domains in polarized cells, FITC-dextran was added to either the upper or lower chamber of Transwell filters. Cells were then placed on ice and washed three times with ice-cold serum-free medium, followed by fixation for 90 min in paraformaldehyde/lysine/periodate fixative (2% paraformaldehyde, 75 mM lysine, 10 mM sodium periodate, 0.0375 M phosphate buffer, pH 6.2). Cells were then washed briefly in PBS, and coverslips or filters were mounted on glass slides in a solution of 50% glycerol/1% *n*-propyl gallate in PBS. For double-labeling experiments, cells were first incubated with FITC-dextran and fixed in paraformaldehyde/lysine/periodate fixative, and then the immunofluorescence procedure was carried out with primary and secondary antibodies as described in the section above. Coverslips were examined with an Olympus microscope fitted for epifluorescence, and cells on filters were examined with a Bio-Rad MRC-600 confocal laser scanning microscope mounted on a Zeiss Axioskop. Intensity measurement values were obtained from confocal microscope images. Image analysis was performed by measuring the total fluorescence intensity using SOM software.

FITC-Transferrin Uptake

MDCK cells grown on semipermeable filters were incubated with serum-free DMEM at 37°C for 1 h followed by a 45-min incubation with DMEM+ in the absence or presence of 1 μM JAS. FITC-transferrin (100 $\mu\text{g/ml}$) in DMEM+ (with or without JAS) was bound to the basolateral cell surface during an incubation on ice for 90 min. Cells were washed three times with ice-cold DMEM+ and then the transferrin was internalized by transferring cells to 37°C for 15 min. Cells were then placed on ice and washed three times in ice-cold PBS+ (PBS containing 1 mM CaCl_2 and 0.5 mM MgCl_2), followed by fixation for 1 h with 4% paraformaldehyde in PBS.

Attached Cell Patches (ACPs)

This method was adapted from a procedure described previously (Robinson *et al.*, 1992). MDCK cells, grown as confluent monolayers on coverslips, were incubated with or without 1 μM JAS for 45 min at 37°C. Coverslips were washed briefly in PBS, followed by a 30-s treatment with 0.5 mg/ml poly-L-lysine in PBS. The cells were swollen by three 2-s incubations in a hypotonic buffer, 1/3 \times buffer A (buffer A: 140 mM KCl, 60 mM HEPES, 10 mM MgCl_2 , 6 mM EGTA, pH 7.5), and sonicated for 4.5 s in buffer B (1 \times buffer A, 1

mM dithiothreitol, 0.1 mM phenylmethylsulfonyl fluoride). Coverslips were fixed in 4% paraformaldehyde in 1 \times buffer A. F-actin was labeled by incubating the coverslips with 2 $\mu\text{g/ml}$ FITC-conjugated phalloidin. This procedure results in extensive disruption of cells, leaving isolated attached cell plasma membrane patches (ACPs) on coverslips.

Detergent Extraction of MDCK Cells

MDCK cells, grown on 100-mm dishes for 3 d, were preincubated with or without 1 μM JAS for 45 min at 37°C. After a brief wash in PBS, 2 ml of 1% Triton X-100 in PBS was added to each dish, and the dish was swirled gently and then left for 2 min at room temperature. The Triton X-100-soluble cell extract was then removed and SDS-PAGE sample buffer was added. The remaining Triton X-100-insoluble cell material was washed in PBS and then solubilized in SDS-PAGE sample buffer. Both fractions were loaded on a 10% SDS-PAGE gel. Proteins were then detected by staining the gel with 0.1% Coomassie blue.

Horseshoe Peroxidase (HRP) Uptake and Electron Microscopy

Uptake of the fluid-phase marker HRP was examined by biochemical and electron microscopic procedures. Cells grown on filters for 3 to 4 d were washed with DMEM+ then preincubated with or without 1 μM JAS for 45 min at 37°C. Cells were incubated with 10 mg/ml HRP type II (Sigma, St. Louis, MO) in the apical or basal medium, in the absence or presence of JAS, for between 0 and 120 min. For biochemical assays, cells were cooled to 4°C and washed three times for 10 min with ice-cold PBS+. Cells were scraped off the filters into PBS containing 0.2% Triton X-100 and left on ice for 30 min. After a brief spin, the cell extract was assayed for HRP activity by using the Sigma Fast OPD peroxidase substrate tablet set and read at an absorbance of 450 nm. Resultant HRP concentrations were normalized by using protein concentrations of the cell extracts. For electron microscopy, cells with ingested HRP were washed in the above buffer and then fixed in 2.5% glutaraldehyde in 50 mM cacodylate buffer. HRP was visualized with diaminobenzidine and the cells were processed for Epon embedding and sectioned as described (Parton *et al.*, 1989). Thin sections were viewed and photographed on a Jeol 1010 electron microscope. The point-counting method (Weibel, 1980) was used to quantitate the amounts of HRP uptake in control and JAS-treated cells. The size of HRP-labeled endocytic compartments (control, $n = 51$; JAS, $n = 64$) and the area of labeled compartments per area of cell (density: control, $n = 136$; JAS, $n = 101$) were compared on a series of micrographs.

RESULTS

JAS Binds to and Stabilizes F-Actin Polymers in Intact Cells

Living cells were treated with the drug JAS to investigate the role of F-actin in the endocytic pathway in polarized and nonpolarized cells. In the experiments reported herein, cells were typically treated with 1 μM JAS for 45 min. These conditions were found, in our hands and by others (Bubb *et al.*, 1994), to produce the maximal detectable effects of JAS without adversely affecting gross cell shape or adherence. To demonstrate JAS binding to F-actin, FITC-phalloidin was used to competitively label actin filaments in MDCK cells that had been treated with JAS prior to fixation and staining. A decreased level of FITC-phalloidin labeling in JAS-treated cells was taken to indicate the

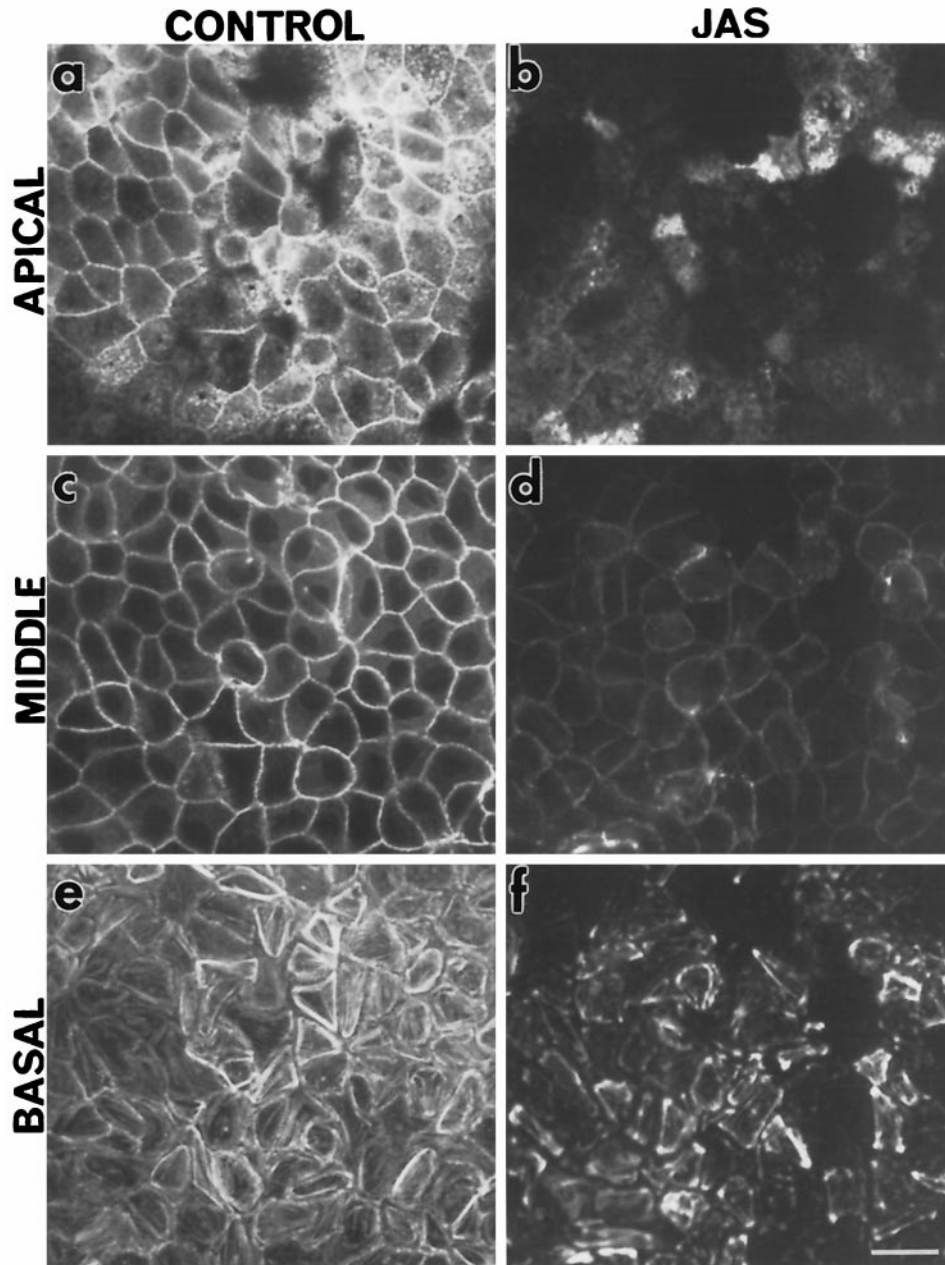


Figure 1. Actin staining in JAS-treated cells. FITC-phalloidin labeling on control and JAS-treated polarized MDCK cells. Confocal microscopy of FITC-phalloidin labeling in nontreated MDCK cells (a, c, and e) and cells pretreated with 1 μ M JAS for 45 min at 37°C (b, d, and f). Typical patterns of labeling for F-actin in the apical terminal web (a), around the midcell cortical web (c), and in stress fibers at the base of cells (e) were seen in control cells. JAS competed with phalloidin binding sites resulting in less-intense labeling at all levels (b, d, and f) of the cell monolayer. Bar, 10 μ m.

presence of bound JAS on F-actin (Bubb *et al.*, 1994; Senderowicz *et al.*, 1994). Decreased FITC-phalloidin labeling was noted at all levels through JAS-treated MDCK cells (Figure 1, b, d, and f) compared with control cells (Figure 1, a, c, and e) examined by confocal microscopy, indicating that JAS had accessed and bound to F-actin at all levels through the cells. There was slightly more FITC-phalloidin labeling in the basal region of JAS-pretreated cells than at other levels, reflecting incomplete saturation of F-actin in

the larger stress fibers by JAS in this region of the cell (Figure 1f).

JAS treatment increased the density of polymerized actin in stress fibers exposed on the cytoplasmic face of plasma membranes in ACPs made from MDCK cells (Figure 2, a and b). As shown above (Figure 1), JAS does not saturate the binding sites on basal cell stress fibers, allowing additional staining of these actin bundles with FITC-phalloidin. Such staining on ACPs showed that the stress fibers in patches from

JAS-treated cells were thicker and more dense than those from control cells, consistent with JAS increasing polymerization of F-actin in these bundles (Figure 2b). JAS also increased the proportion of insoluble F-actin recovered in 1% Triton X-100 extracts of MDCK cells. Proteins in the detergent-soluble and -insoluble fractions of untreated and JAS-treated MDCK cells were analyzed by SDS-PAGE. The abundant actin protein band (at ~42 kDa) could be readily seen on Coomassie blue-stained gels (Figure 2c) and its identity was further verified by immunoblotting with an actin antibody (our unpublished results). In extracts of control cells, actin was present in both detergent-soluble and -insoluble fractions (Figure 2c), whereas after JAS treatment, there was no actin remaining in a soluble form and all of it was recovered as F-actin in the insoluble fraction (Figure 2c). Thus, these data indicate that JAS is effectively inducing the formation of and/or stabilizing existing F-actin in intact cells.

Effect of JAS on FITC-Dextran Uptake in Nonpolarized MDCK Cells

FITC-dextran was used as a fluorescent marker of fluid-phase endocytosis. The effect of JAS on FITC-dextran uptake was examined at various times between 5 and 60 min of uptake in nonpolarized (preconfluent) MDCK cells grown on coverslips (Figure 3). The most distinct difference between control and JAS-pretreated cells was seen at 15 min and 30 min, although there were also differences in their staining patterns noted at earlier times. There was an increase in the number and, particularly in the size, of FITC-labeled structures in the JAS-treated cells compared with those seen in control cells after 15 min of uptake (Figure 3). After 30 min of uptake, the distinct punctate labeling seen throughout both control and pretreated cells was more prominent and abundant after JAS treatment (Figure 3). JAS appears to have increased the uptake and/or retention of FITC-dextran in nonpolarized MDCK cells.

JAS Does Not Affect Apical Endocytosis in Polarized Cells

To study the effects of JAS on endocytosis in polarized cells, FITC-dextran uptake was examined by confocal microscopy in confluent monolayers of polarized filter-grown MDCK cells. These polarized cells have distinct apical and basolateral surfaces with characteristic arrays of apical and basal actin filaments (see Figure 1). FITC-staining was examined in confocal-generated Z-series images of cell monolayers after FITC-dextran was added to either the apical or basolateral surface of control or JAS-pretreated cells for various times. Cells were compared at three selected levels: basal (adjacent to the basal plasma membrane), middle (the supranuclear middle region of the cell),

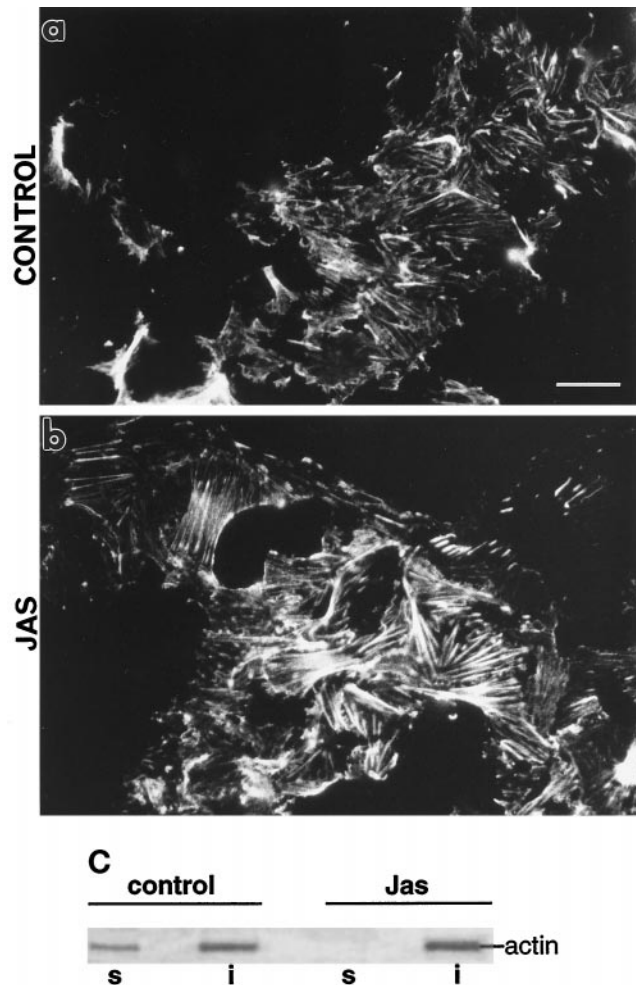


Figure 2. Actin polymerization induced by JAS treatment. (a and b) FITC-phalloidin labeling of actin bundles attached to the cytoplasmic face of ACPs remaining stuck to coverslips after sonication of the MDCK cells. (a) Control cells have labeling of fine bundles of stress fibers. (b) After JAS treatment, there were thicker more-prominent actin bundles. Bar, 10 μ m. (c) Proteins in detergent-soluble and -insoluble fractions of control and JAS-treated MDCK cells were electrophoresed on SDS-PAGE gels and stained with 0.1% Coomassie blue. Left, a 42-kDa band representing actin is present in both the Triton X-100-soluble (lane s) and -insoluble (lane i) fractions of nontreated MDCK cells. Right, the actin band has disappeared from the soluble fraction of JAS-treated cells (lane s) and all of the recovered actin is in the insoluble fraction (lane i), consistent with a conversion to F-actin.

and apical (adjacent to the apical plasma membrane, at the base of the microvilli). By examining time courses of fluid-phase marker endocytosis, we selected these levels to correspond to the preponderance of early endosomes clustered near the cell periphery (apical or basal) and late endosomes or sorting endosomes concentrated in the middle region of the cell. A similar distribution of endocytic structures in MDCK cells has

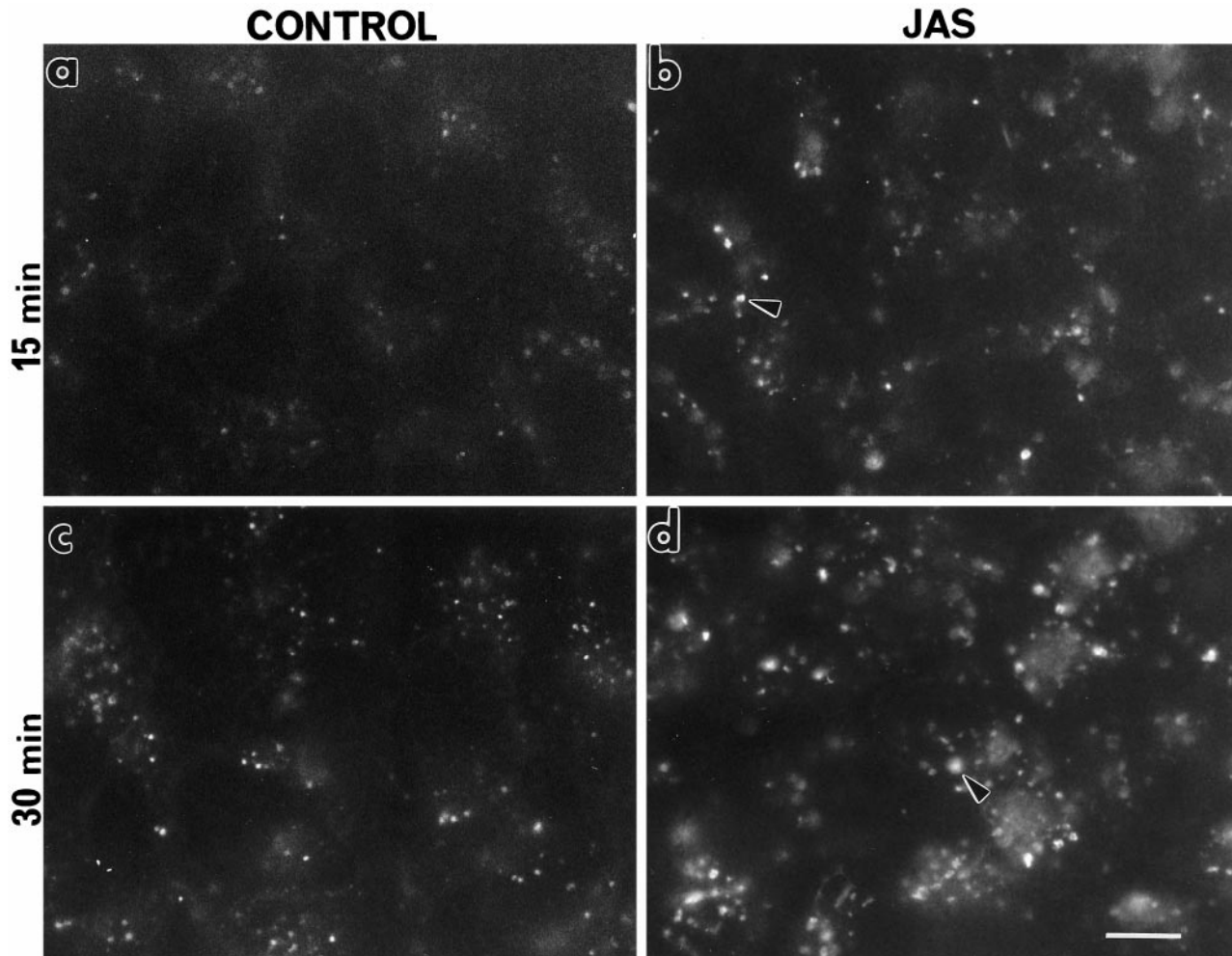


Figure 3. FITC-dextran uptake in preconfluent MDCK cells. Control and JAS-pretreated cells, grown on coverslips, were incubated with FITC-dextran for 15 min or 30 min at 37°C, and the endocytosed marker was visualized by epifluorescence microscopy. After both 15 min and 30 min uptake in JAS-pretreated cells, there was an increase in the number and size of fluorescently labeled compartments (arrows) (b and d) in comparison to those seen in control cells (a and c). Bar, 10 μm .

been established in an earlier study by Bomsel *et al.* (1989).

Figure 4 shows FITC-dextran uptake from apical and basal surfaces after 15 min of uptake. There was consistently more FITC-dextran uptake from the basolateral surface than from the apical side of these MDCK cells (Figure 4, a–c and g–i), as was also noted previously (Bomsel *et al.*, 1989). There was no significant difference recorded for FITC-dextran uptake from the apical side of control or JAS-treated MDCK cells over 5–30 min. Figure 4 demonstrates that at the apical and middle cell levels, there was little difference in labeling between control and JAS-pretreated cells after uptake for 15 min (Figure 4, a, b, d, and e). At the basal region of JAS-pretreated cells, the appearance of some punctate labeling was noticed after addition of the FITC-dextran to the apical medium (Figure 4, c and f).

This we believe is due to some leakage of the apical FITC-dextran into the basal medium where the permeability of the tight junctions is compromised by JAS treatment. Thus JAS-induced actin polymerization did not demonstrably alter fluid-phase uptake at the apical cell membrane.

Actin Polymerization Increases FITC-Dextran Uptake from the Basolateral Domain of MDCK Cells

The basolateral uptake of FITC-dextran in polarized MDCK cells was also examined, and evidence was obtained that JAS treatment had significant effects on basolateral endocytic pathways. Very little FITC-dextran was found in the apical cell sections after a 15-min uptake from the basal side (Figure 4, g and j). Most of

the label in the control cells had accumulated in endocytic structures in the middle cell sections at 15 min (Figure 4h). In JAS-treated cells, the middle cell sections were more heavily labeled and the size of the fluorescently labeled endocytic structures was larger than those in control cells (Figure 4k). In the basal cell region, the number and size of labeled endocytic structures had greatly increased after JAS treatment, compared with control cells (Figure 4, i and l). These results suggest that JAS increased the uptake and/or accumulation of FITC-dextran in endocytic structures concentrated in the basal and middle cell regions.

The effect of JAS on basolateral FITC-dextran uptake was further examined during a time course experiment, the results of which are shown in Figure 5. Because there was little labeling in the apical cell section, only the basal and middle sections of the cells are shown. During longer times of uptake, there was a progressive increase in the uptake and delivery of FITC-dextran to the middle of the cells in both control and JAS-treated cells. After 7.5 min of uptake in JAS-pretreated cells, there were more numerous and larger endocytic structures labeled with FITC-dextran at the basal region but less labeling in the middle region compared with controls (Figure 5, a–d). Thus, although there was more uptake in JAS-treated cells, the label in control cells was initially more efficiently transported to the middle cell regions. At 15 and 30 min, the labeled endosomes were progressively larger and more numerous after JAS treatment (Figure 5, f, h, j, and l, and see Figure 4).

The amount of FITC-dextran labeling in the basal or middle cell regions at 15 min was quantified and compared by image analysis (Figure 6). We found that the labeled structures could be separated into two distinct populations according to fluorescence intensity; a population of small round endocytic structures (small endosome clusters) and a population of larger very intensely labeled compartments (large endosome clusters). Confocal images of these pseudocolored compartments were analyzed by measuring the relative fluorescence intensity (pixels per area) using SOM software (Figure 6, a and b). An example of one of these colored images shows that “small endosome clusters” are present and abundant in treated and untreated cells (Figure 6, a and b; green), whereas “large endosome clusters” are much more abundant in JAS-treated cells (Figure 6b; red). Cumulative measurements of both basal and middle regions shows that JAS induced more than a twofold increase in total FITC-dextran accumulation (Figure 6c). In the basal region, JAS increased labeling by fivefold, but in the middle region, it caused a less dramatic increase in FITC-dextran labeling. Separate analysis of accumulation in small or large endosome clusters is also shown in Figure 6c. The large clusters are almost absent from the basal region of control cells and are present mostly

in the middle region. In JAS-treated cells, large endosome clusters are now present in both the basal cell region and more of them are present in the middle of the cell. The number of small clusters in the basal region is increased by fivefold in JAS-treated cells (Figure 6c). These analyses reveal that JAS-induced actin polymerization increases the uptake and accumulation of FITC-dextran in small basally located endosomes and in clusters of larger perinuclear (middle region) endosomes. It is likely that JAS affects uptake or transport of FITC-dextran at both early and late stages of endocytosis. The JAS-induced appearance of more of the large endosome clusters after 15 min of uptake prompted further investigation of this compartment. Two further approaches, described below, were taken to characterize the endocytic compartments affected by JAS.

JAS Has No Effect on the Basolateral Uptake and Recycling of FITC-Transferrin

To investigate the effect of actin polymerization on the receptor-mediated endocytic pathway, we examined the uptake of FITC-transferrin in the presence of JAS. Small punctate endocytic compartments, labeled with the fluorescent marker, were observed close to the basolateral cell surface in both control and JAS-treated cells (Figure 7, a and b). JAS did not cause an increase in the uptake or accumulation of FITC-transferrin as measured by confocal analyses.

Effects of JAS on HRP Uptake

Uptake experiments on polarized MDCK cells were repeated with the electron-dense fluid-phase marker HRP. First, a biochemical assay was used to measure HRP uptake over a time course of 0–120 min. JAS pretreatment had no effect on HRP uptake from the apical domain (Figure 8A), but it significantly increased uptake from the basolateral surface (Figure 8, B and C). Basolateral HRP uptake in JAS-treated cells during a continuous labeling protocol showed a steady accumulation of HRP, consistently higher at all time points than in untreated cells (Figure 8b). A pulse–chase labeling protocol showed that the initial uptake of HRP was greatly increased by JAS, that there was some loss of HRP due to recycling within the first 60 min, and that thereafter there was a steady accumulation of HRP (Figure 8C). These results are consistent with an increased uptake of HRP and its sequestration at higher levels in late endocytic compartments in JAS-treated cells.

The HRP-labeled compartments were examined at an ultrastructural level in cells fixed and embedded after the HRP uptake for 15 min (Figures 9 and 10). The majority of HRP-labeled endosomes were found in the supranuclear region of the cells, at an equivalent level to the middle level analyzed by confocal micros-

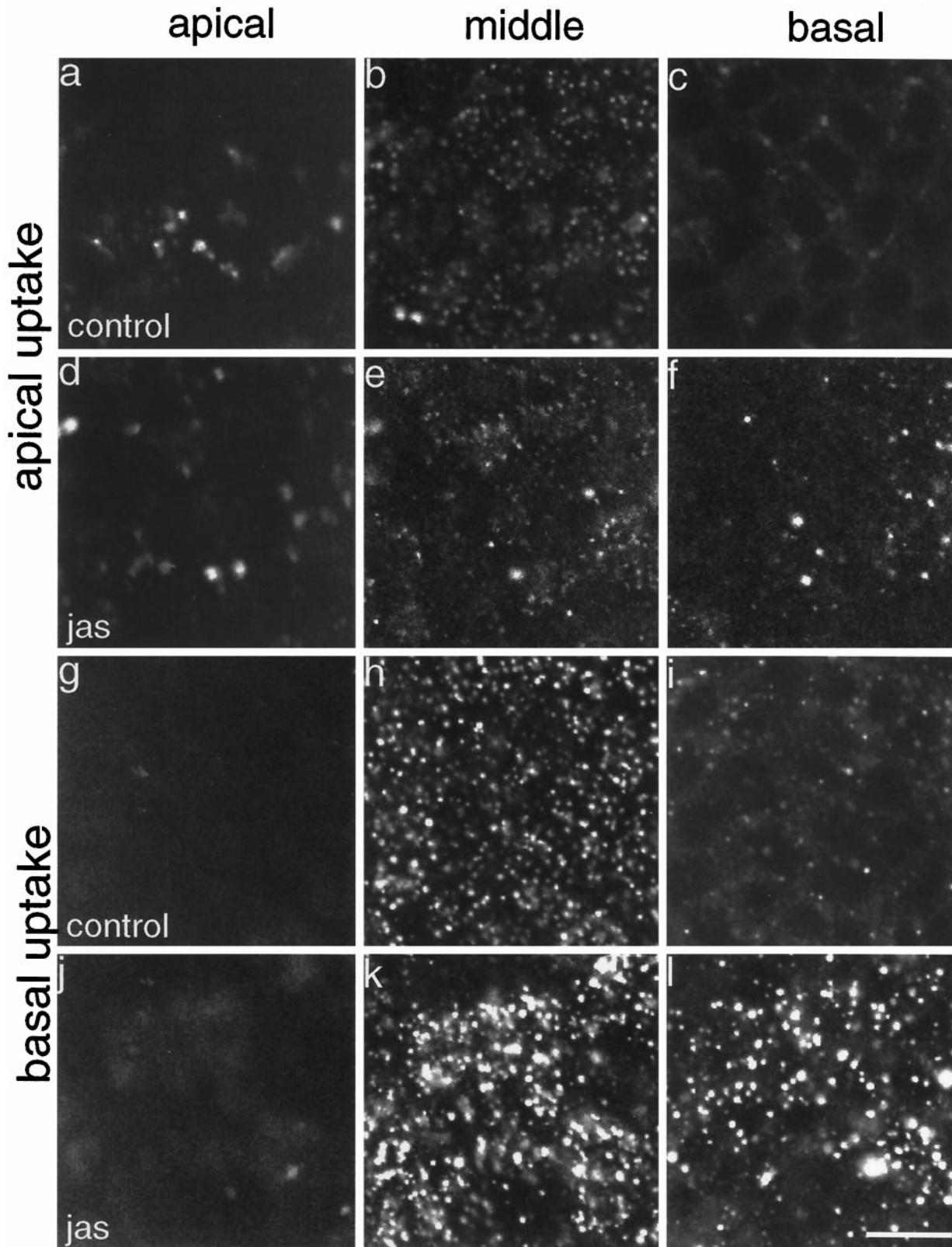


Figure 4.

copy. The labeled endosomes at the basal cell poles were dispersed and harder to quantify in thin sections, and there were virtually no HRP-labeled endosomes at the apical level, consistent with the distribution of FITC-dextran labeling. In JAS-treated cells, there were more HRP-labeled endosomes and many of them were densely clustered within the supranuclear regions of the cells (Figure 10, B and C). At this time point, many of the HRP-labeled structures had the appearance of late endosomes/lysosomes in that they were large, many had tubular extensions, and some were multivesicular.

HRP uptake was quantified by a point counting method that confirmed that the relative density of the HRP-labeled compartments in JAS-pretreated cells was double that of control cells (Figure 9A). Point counting on multiple sections through the middle regions of cells showed an increased amount of HRP labeling per unit area in JAS-treated cells. However, the size of individual endosomes was not increased by JAS treatment and there was no evidence that JAS induced abnormal fusion of endosomes (Figure 9B). At the electron microscope level, we observed that the large endosome clusters labeled with FITC-dextran are groups of densely packed large (late) endosomes (Figure 10c), whereas smaller (early) endosomes that were less tightly packed accounted for small endosomes clusters. Overall the results of the HRP-uptake corroborate the results obtained with FITC-dextran uptake, showing that JAS-induced actin polymerization increases both the uptake and accumulation of fluid-phase markers from the basolateral cell surface. After 15 min of uptake, JAS-treated cells had accumulated increased numbers of clustered compartments with the appearance of late endosomes.

JAS Induces Apical Membrane Bunching

The morphology of JAS-treated cells was also examined at the ultrastructural level. The morphology of the filter-grown MDCK cell monolayers was largely unchanged by JAS treatment and the cells maintained their characteristic polarized morphology. The only dramatic difference noted in JAS-treated cells was an

unusual bunching of the apical cell surface. In control cells the MDCK apical membrane was flat with a continuous linear array of microvilli, whereas in JAS-treated cells the whole apical membrane was drawn together, or bunched, with all of the membrane gathered into one tuft (Figure 10B). These apical bunches contained all of the microvilli, which were shortened, with coated pits at their bases; however, the bunches were devoid of other intracellular organelles (Figure 10, A and B). Dense patches of actin filaments could be seen in some micrographs in the apical bunches. This unusual apical bunching was noted in all of the JAS-treated MDCK cells, although its significance with respect to membrane trafficking was not investigated further.

JAS and Nocodazole Have Distinct Effects on Basolateral Endocytosis

Disruption of microtubules with nocodazole has been shown to inhibit transport of endocytosed markers from early to late endosomes (Gruenberg *et al.*, 1989). To compare the steps of endocytosis affected by actin polymerization and microtubule depolymerization, FITC-dextran uptake was compared in JAS-treated and nocodazole-treated cells. Treated MDCK cells were examined after a time course of uptake; the results in Figure 11, showing FITC-dextran labeling within the middle (Figure 11, a and b) and basal cell regions (Figure 11, c and d), indicate that FITC-dextran is accumulated in different compartments after either JAS or nocodazole treatments. In nocodazole-treated cells, the marker is taken up basally (Figure 11d) but is not transported to the interior of the cell or does not appear in larger endosomes (Figure 11b), consistent with a block in transport early in the endocytic pathway. JAS-treated cells show the characteristic accumulation of FITC-dextran in larger structures in the supranuclear position (Figure 11a). JAS-induced actin polymerization accumulates fluid-phase marker later in the endocytic pathway than the microtubule-dependent early-late endosome transition.

Accumulated FITC-Dextran Does Not Colocalize with Other Organelle Markers

In an attempt to identify the late endocytic compartments accumulated by JAS treatment, cells were double-labeled for FITC-dextran and a variety of antibodies to organelle markers for the endocytic pathway. FITC-dextran in the clustered compartments (large endosome clusters) induced by JAS did not colocalize with any of the markers used (Figure 12). A marker of early endosomes, rab5, was found in small intracellular punctate structures particularly in the apical cell periphery of JAS-treated MDCK cells (Figure 11, a and b). The late endosome markers rab7 and mannose-6-phosphate receptor (M6PR) were concentrated in

Figure 4 (facing page). FITC-dextran uptake in polarized cells. Control and JAS-pretreated cells, grown on filters, were incubated with FITC-dextran added to either the apical or basolateral chamber for 15 min. Confocal microscopy shows endocytosed label at designated levels representing apical, middle, and basal levels of the cell monolayer. Little label was endocytosed from the apical side of either control (a–c) or JAS-treated (d–f) cells. A large amount of FITC-dextran was taken up from the basal medium and it was sequestered in structures at the basal and middle planes of control (h and i) and JAS-treated (k and l) cells. There was a marked increase in the number and size of labeled endocytic compartments in both the middle (k) and basal (l) planes after JAS treatment. Bar, 10 μ m.

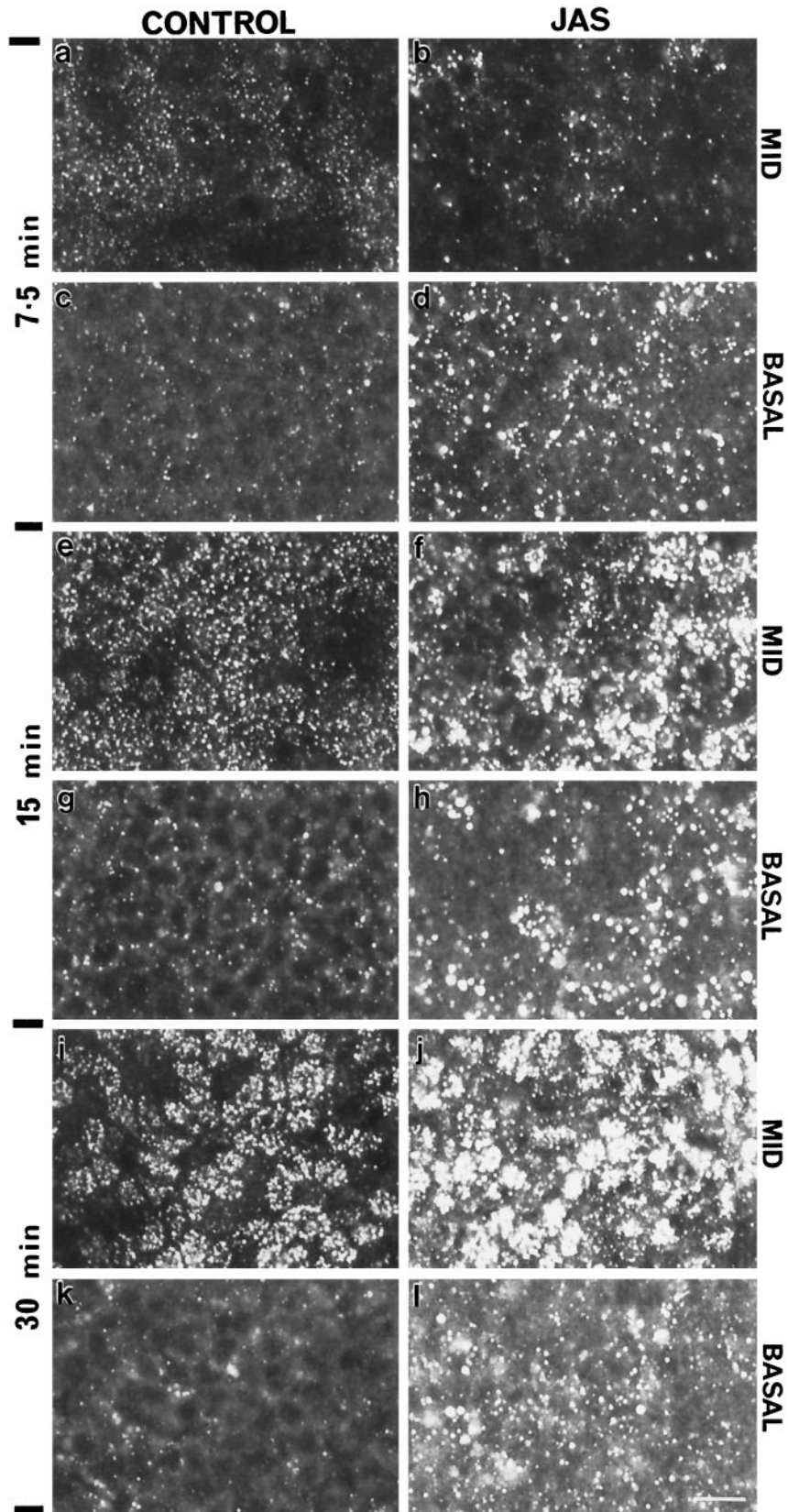


Figure 5.

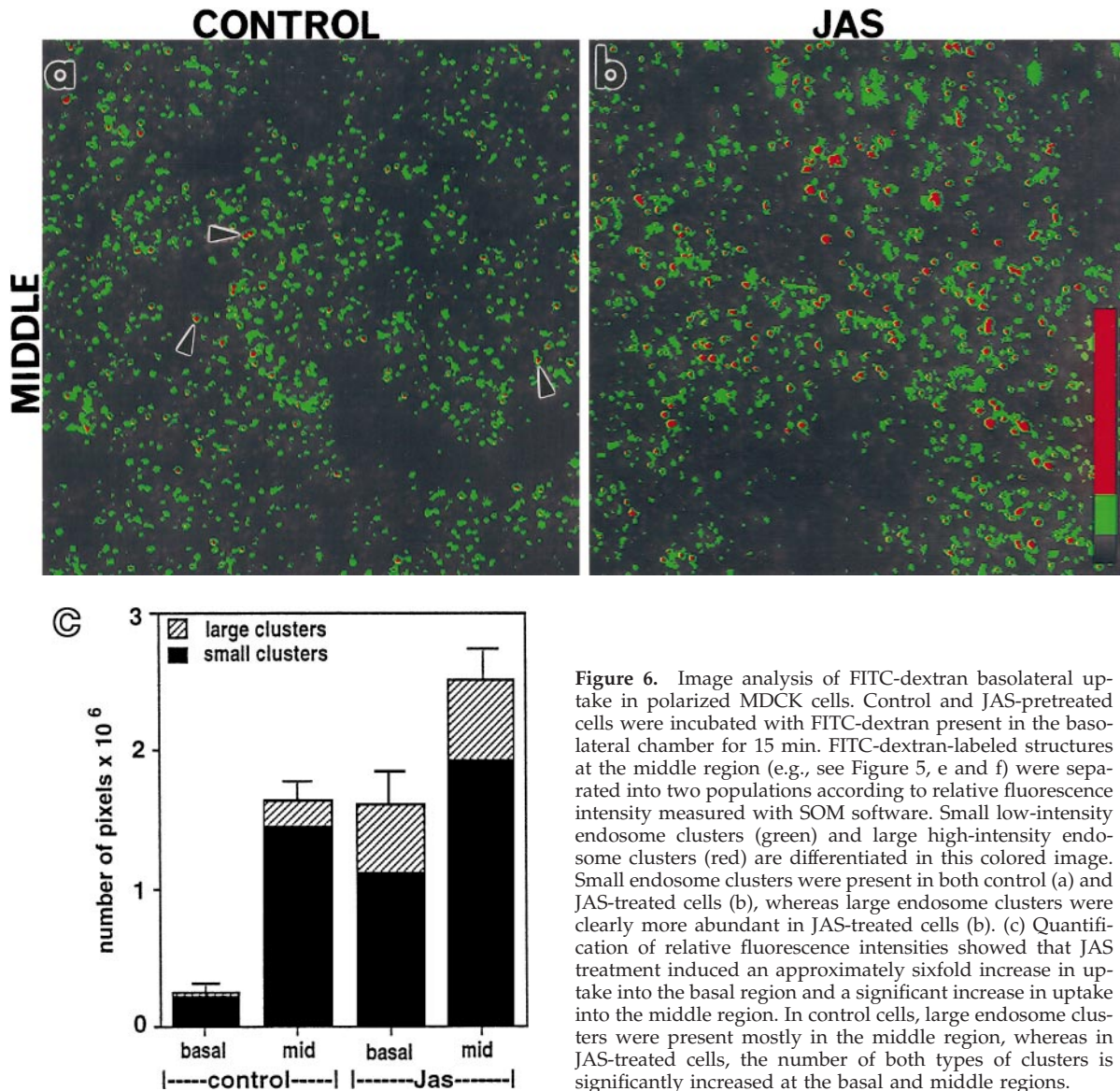


Figure 6. Image analysis of FITC-dextran basolateral uptake in polarized MDCK cells. Control and JAS-pretreated cells were incubated with FITC-dextran present in the basolateral chamber for 15 min. FITC-dextran-labeled structures at the middle region (e.g., see Figure 5, e and f) were separated into two populations according to relative fluorescence intensity measured with SOM software. Small low-intensity endosome clusters (green) and large high-intensity endosome clusters (red) are differentiated in this colored image. Small endosome clusters were present in both control (a) and JAS-treated cells (b), whereas large endosome clusters were clearly more abundant in JAS-treated cells (b). (c) Quantification of relative fluorescence intensities showed that JAS treatment induced an approximately sixfold increase in uptake into the basal region and a significant increase in uptake into the middle region. In control cells, large endosome clusters were present mostly in the middle region, whereas in JAS-treated cells, the number of both types of clusters is significantly increased at the basal and middle regions.

punctate structures in the supranuclear region, but these structures labeled with these antibodies did not coincide with the large endosome clusters containing FITC-dextran in the JAS-treated cells (Figure 12, c–f).

Figure 5 (facing page). Kinetics of FITC-dextran uptake from the basal side of MDCK cells. The middle and basal planes of control and JAS-treated MDCK cells were examined by confocal microscopy after uptake of FITC-dextran for 7.5, 15, and 30 min. JAS-pretreated induced an increase in the number and size of labeled compartments at the basal region at all times (d, h, and l) compared with control cells (c, j, and k). JAS also produced an increase in labeled compartments in the middle region of the monolayer at the later times of 15 (f) and 30 min (j), when compared with control cells after the same uptake times (e and i). Bar, 10 μm .

TRITC-transferrin, bound to the basolateral cell surface, was simultaneously taken up into cells with FITC-dextran for 15 min. Most of the transferrin in cells was then found in basolateral early endosomes and in the apical region where it was possibly labeling the apical recycling compartment. There was not widespread colocalization of FITC-dextran and transferrin after a 15-min uptake (Figure 12, g and h), although occasional JAS-treated cells showed double-labeled endosomes in the basolateral region (Figure 12h). As a fluid-phase marker, FITC-dextran is endocytosed via multiple pathways, and the bulk of its uptake is likely to occur through clathrin-independent pathways. These experiments suggest that JAS treatment increases the uptake of FITC-dextran and accu-

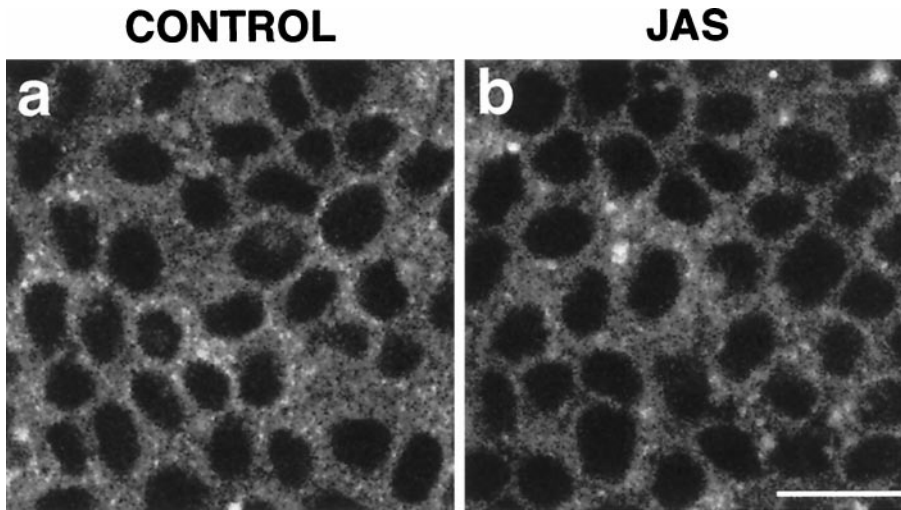


Figure 7. FITC-transferrin uptake. FITC-transferrin was bound to the basolateral surface of control (a) and JAS-pretreated (b) MDCK cells at 4°C and then internalized for 15 min at 37°C. Small punctate FITC-transferrin-labeled compartments were present at similar levels in the basolateral cell periphery of both control (a) and JAS-pretreated (b) cells. Bar, 10 μ m.

multates this marker in endosomes, particularly in late macropinocytic endosomes that are distinct from other late endosomes labeled for rab7 and M6PR.

DISCUSSION

Several previous lines of evidence, gathered mostly from the use of actin-depolymerizing drugs or expression of actin-binding proteins, suggest that actin filaments are involved in endocytic pathways. The drug JAS has an action similar to phalloidin in binding to and stabilizing F-actin, with the added advantage of being cell permeant. Our studies on intact cells demonstrate a novel use of JAS to induce actin polymerization for studies on endocytosis. Our data demonstrate that polymerization of actin enhances the uptake and accumulation of fluid-phase markers in endocytic compartments. Moreover, JAS had its most pronounced effect on uptake from the basolateral domain of polarized MDCK cells, thus newly implicating actin in endocytic processes at the basolateral pole of epithelial cells.

JAS-induced actin polymerization increased the basolateral uptake of the fluid-phase markers FITC-dextran and HRP, which enter cells through multiple pathways, including the clathrin-mediated endocytic pathway and several clathrin-independent pathways, including macropinocytosis (von-Bonsdorff, *et al.*, 1985; Bomsel *et al.*, 1989; Parton *et al.*, 1989; Brown and Sabolic, 1993; Hewlett *et al.*, 1994; Thilo *et al.*, 1995; Futter *et al.*, 1996). The uptake of both fluid-phase markers was initially significantly increased in JAS-treated cells and thereafter there was a steady accumulation of markers at all time points. After JAS treatment, some of the internalized HRP (~20%) in pulse-labeled cells was recycled out of the cell, showing that JAS does not impair, and may even enhance, early

recycling events and that the remaining HRP accumulated in the cell. The dynamics of HRP uptake measured herein are consistent with findings that most of the cell membrane endocytosed by various pathways is recycled from an early endocytic compartment (Mayor *et al.*, 1993), whereas the bulk of fluid-phase markers are generally processed through lysosome-directed pathways without much immediate recycling (Parton *et al.*, 1989; Hewlett *et al.*, 1994; Futter *et al.*, 1996). In contrast, JAS did not affect the uptake or early recycling of FITC-transferrin, consistent with other studies using cytochalasin D or phalloidin that did not affect this pathway (Lamaze, *et al.*, 1996; Maples *et al.*, 1997). JAS-induced actin polymerization may, therefore, primarily effect clathrin-independent endocytosis. The transient colocalization of internalized TRITC-transferrin and FITC-dextran does suggest that some fluid-phase uptake in these cells passes through early compartments of the receptor-mediated pathway but the bulk of the fluid-phase markers were obviously internalized by other actin-sensitive pathways.

At later stages of endocytosis, JAS caused a progressive accumulation of fluid-phase markers and a notable clustering of the more numerous labeled compartments. JAS may be influencing several stages of transfer between endocytic compartments. Transport between early and late endosomes is a microtubule-dependent step and disruption of this step with nocodazole accumulates markers in a distinctive compartment (Gruenberg *et al.*, 1989; Parton *et al.*, 1989). In comparing the accumulation of FITC-dextran under various treatments, it was clear that actin polymerization was not disrupting this same microtubule-dependent step, because the labeling patterns produced by JAS and nocodazole were distinct. JAS appears to cause accumulation in later endocytic compartments.

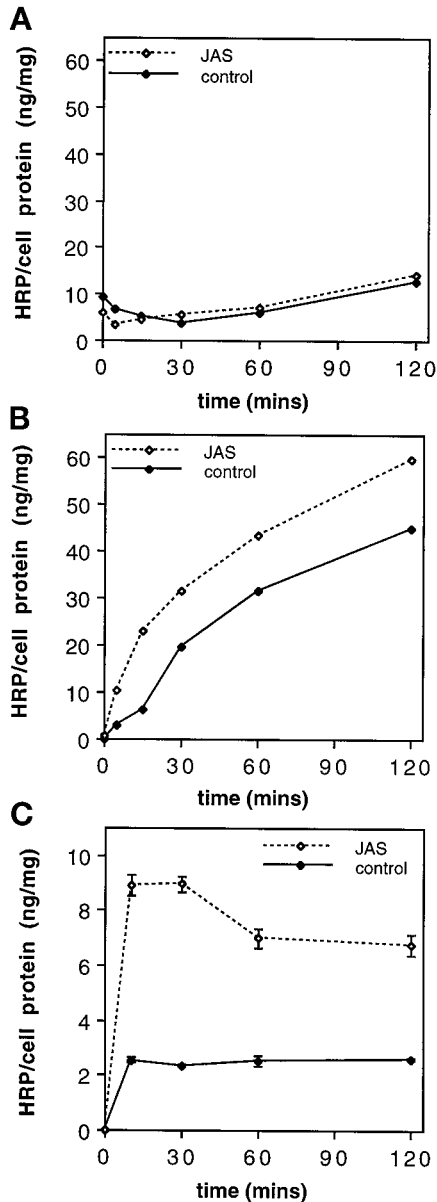


Figure 8. HRP uptake and accumulation. Control and JAS-treated cells were incubated with HRP added to the apical (A) or basolateral (B) chamber over a time course (0, 5, 15, 30, 60, and 120 min) for continuous labeling or added to the basolateral chamber in a pulse-chase regime for 10 min followed by chase incubations of 20, 50, and 110 min (C). HRP uptake values were determined by measuring the HRP activity present in the cell lysate of each filter-grown monolayer and were normalized to the protein concentration of each sample. JAS pretreatment increased the uptake of HRP from the basolateral cell surface at all time points (B) compared with uptake in control cells but had no effect on the apical uptake of HRP (A). Pulse-chase labeling (C) shows an initial increased uptake in JAS-treated cells, followed by a loss of HRP (recycling) during the first 60 min and then sustained accumulation at a higher level than control cells. Points in A and B represent the average of two values (i.e., two filters). In graph C, each data point is the mean and SEM of four samples.

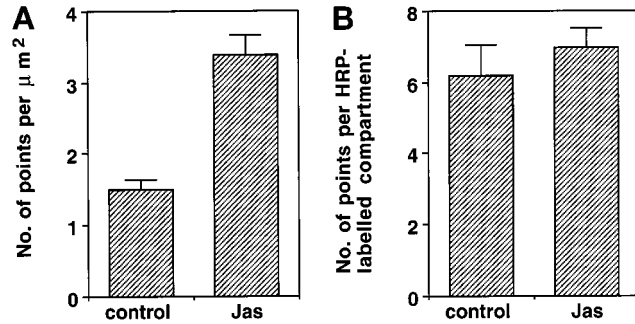


Figure 9. Comparison of HRP uptake in control and JAS-treated cells by electron microscopy. The area of HRP-labeled structures was quantitated by point counting in defined areas on micrographs of the supranuclear region of the cells. Analysis showed that the relative density of HRP-labeled compartments in JAS-pretreated cells was more than twofold that of control cells (A). There was no significant difference in the size of individual HRP-labeled compartments between control and JAS-pretreated cells (B).

In contrast, cytochalasin D has been reported to affect an early endocytic event, one prior to the nocodazole step in transcytotic pathways in polarized cells (Maples *et al.*, 1997). Interestingly, in receptor-mediated endocytosis (Durrbach *et al.*, 1996b) and in the fluid-phase uptake measured herein, the early and late steps involving F-actin appear to flank an intermediate step that is controlled by microtubules.

The large endosome clusters defined herein by FITC-dextran labeling were increased in number in JAS-treated cells after 15–30 min of uptake. By electron microscopy, many of the HRP-labeled compartments had the appearance of late endosomes or lysosomes as tubulated or multivesicular compartments in the perinuclear area. The position and appearance of these compartments are consistent with late or sorting endosomes reported in MDCK cells that receive both apically and basolaterally endocytosed markers from early endosomes (Parton *et al.*, 1989). However, unlike previous studies (Parton *et al.*, 1989), these compartments were not colabeled for other late endosome markers such as M6PR or for rab7. In other cells types, the bulk of fluid-phase markers are taken up by macropinocytosis and delivered to a distinct late endosome that is not colabeled for M6PR (Hewlett *et al.*, 1994). The persistent presence of large amounts of HRP in late endocytic compartments in JAS-treated cells suggests that transfer of HRP between late endosomes and lysosomes was impaired by actin polymerization. This was not, however, tested directly because HRP is not degraded efficiently in lysosomes and delivery to this compartment is difficult to measure. The compartments accumulating markers in JAS-treated cells require further characterization; they might belong to a pinocytic pathway or may be transport intermediates of better known pathways.

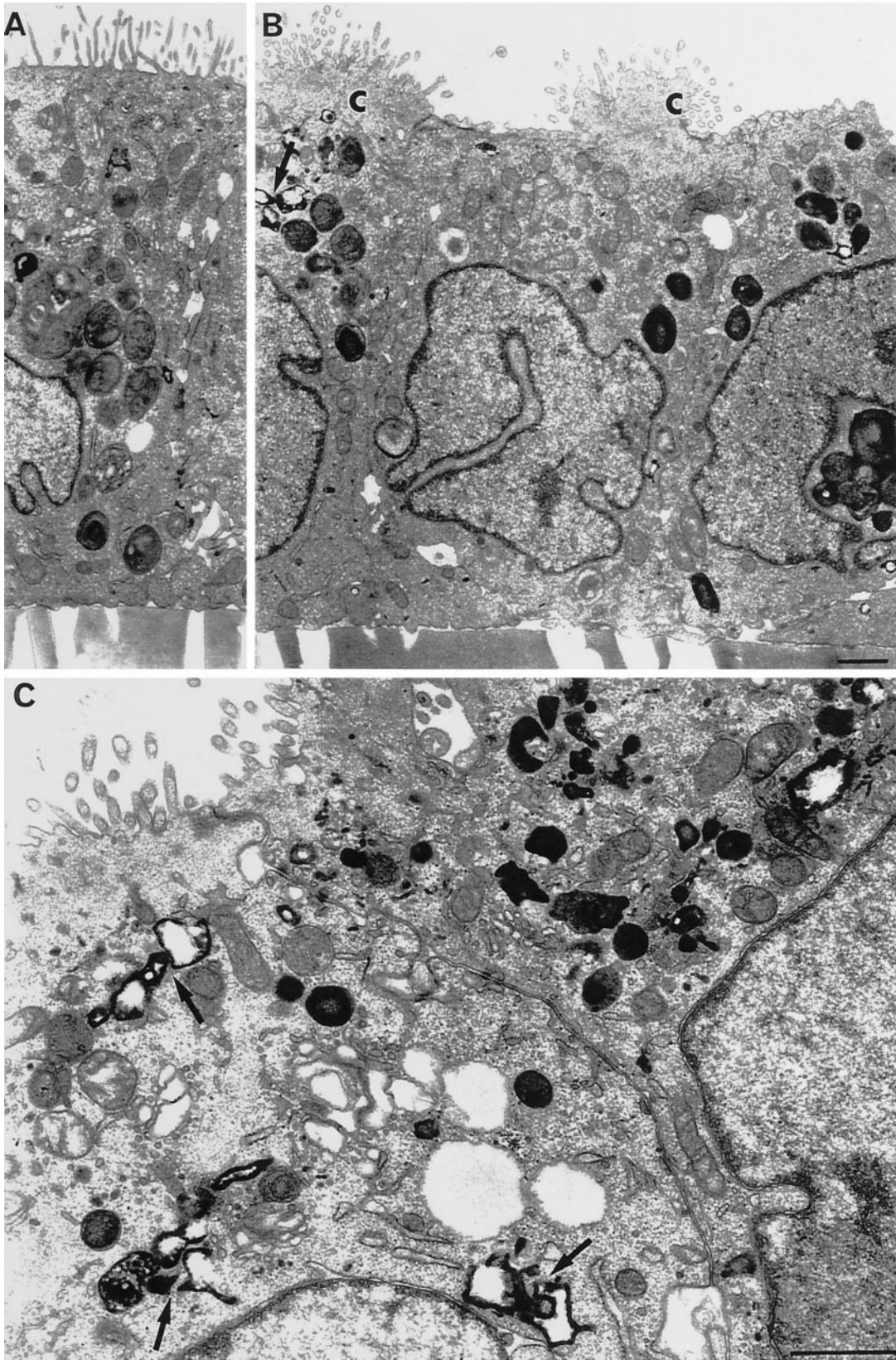


Figure 10.

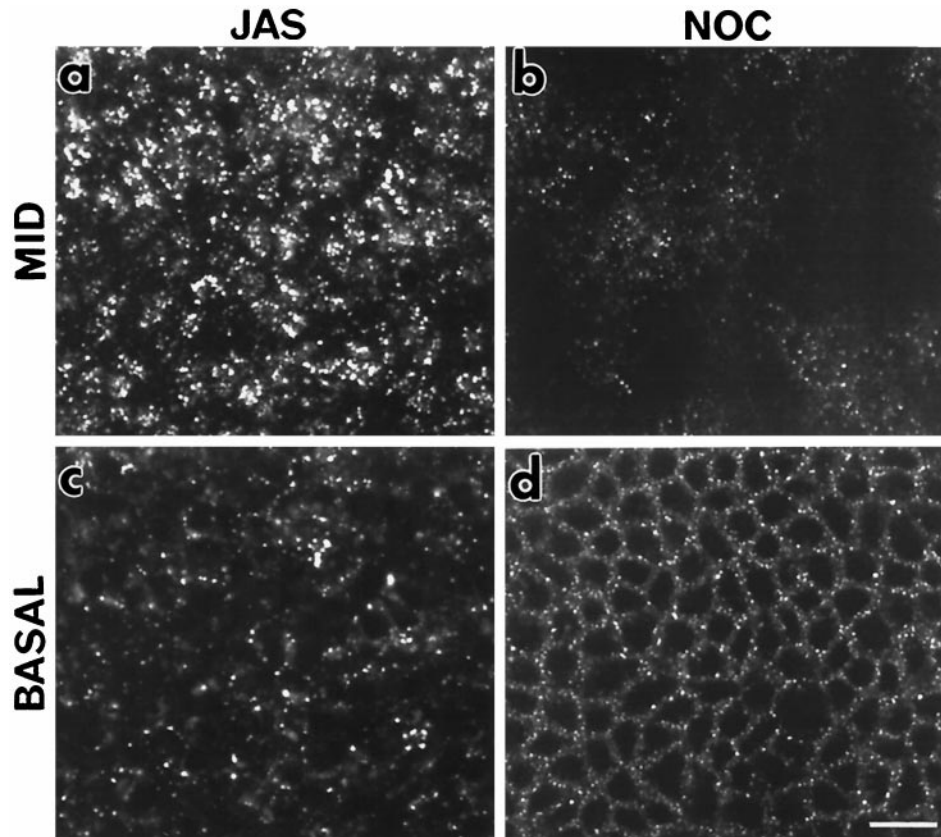


Figure 11. Effects of JAS and nocodazole on FITC-dextran uptake. FITC-dextran uptake was compared in JAS- and nocodazole-treated MDCK cells incubated with FITC-dextran in the basolateral chamber for 15 min. In JAS-treated cells, large characteristic labeled structures were present at the middle (a) and basal (c) region of the monolayer. In nocodazole-treated cells, FITC-dextran-labeled compartments were present at the basolateral cell periphery (d). In contrast to JAS-treated cells, there were less labeled compartments in the supranuclear region of nocodazole-treated cells (b), the labeled endocytic vesicles being smaller and more uniform in size (b and d). Bar, 10 μm .

The distribution of endocytic organelles and their movement toward the perinuclear area has been previously attributed to interaction with microtubules (Matteoni and Kreis, 1987). Actin filaments have an additional role in the organization of endocytic structures and pathways. Depolymerizing actin filaments scatters perinuclear endocytic compartments (Durrbach *et al.*, 1996b), and inducing actin polymerization had the effect of clustering or pulling them together. Similarly, actin filaments have been shown to facilitate the perinuclear clustering of mature endosomes and their fusion with lysosomes (van Deurs *et al.*, 1995). One of the most notable effects of JAS treatment was

the clustering of labeled large or late endosomes in the perinuclear area, providing further evidence that actin filaments can control the cytoplasmic distribution of these organelles. We found no evidence of fusion induced by actin polymerization; when measurements were carried out, there was no increase in the size of individual HRP-labeled endosomes. The HRP-labeled endosomes did have a particularly tubular appearance compared with endosomes in control cells, further supporting the theory advanced by others that tubular extensions or sorting extensions are drawn out along actin filaments assembled around the endosome surface (Durrbach *et al.*, 1996b; Murphy *et al.*, 1996). In the presence of JAS, which stabilizes actin in a polymerized state, the endosomes may be “frozen” in this configuration.

The effects of JAS were examined on polarized MDCK cells in monolayers. Endocytic pathways at the two domains of polarized cells can be structurally and functionally different and may vary between cell types. The transferrin receptor is found predominantly at the basolateral domain of epithelial cells (Fuller and Simons, 1986) where it is endocytosed via a clathrin-dependent process. Ricin, a general membrane marker, shows that internalization occurs pri-

Figure 10 (facing page). HRP labeling and morphology of polarized MDCK cells. The ultrastructure of control (A) and JAS-treated (B and C) MDCK cells was examined after 15 min of HRP uptake from the basolateral side. All cells appeared as polarized monolayers with internalized HRP in a variety of compartments throughout endocytic pathways. Labeled structures were concentrated in the supranuclear or middle cell regions and were particularly prominent in JAS-treated cells, where they can be seen as clusters of tubular or multivesicular endocytic compartments containing HRP (arrows; B and C). In B, the apical microvillar surfaces of JAS-treated cells can be seen gathered up into prominent bunches (C), which were not present in control cells. Bar, 1 μm .

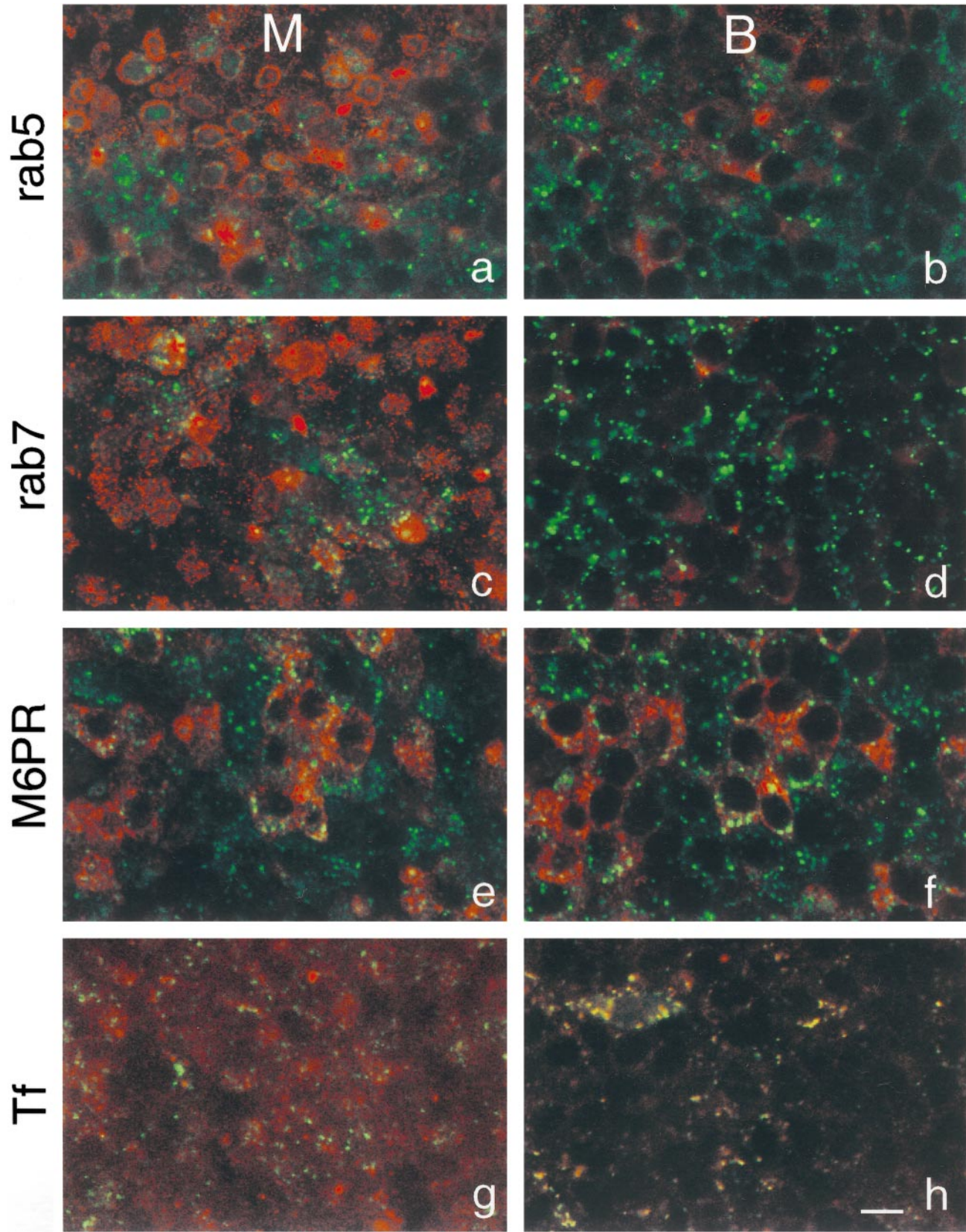


Figure 12.

marily through clathrin-coated pits at the apical domain of polarized Caco-2 cells (Shurety *et al.*, 1996), whereas both clathrin-dependent and -independent pathways have been shown to present at the apical domain of MDCK cells (Eker *et al.*, 1994). Measurements of the uptake of fluid-phase markers in polarized MDCK cells show that the rates of endocytosis at the apical and basolateral domains are equivalent, although the total amount of endocytosis from the basolateral domain is approximately six times greater, proportional to its larger surface area (von-Bonsdorff *et al.*, 1985; Bomsel *et al.*, 1989). Similarly, in the present study, FITC-dextran and HRP were found to be endocytosed more efficiently from the basolateral surface than from the apical surface in MDCK cells. Polymerization of actin with the cell-permeant drug JAS has demonstrated a role for F-actin in the endocytic pathway from the basolateral cell surface in polarized cells. Our results provide evidence for a role of actin in basolateral uptake that are similar to those of a study on transcytosis of polymeric Ig receptor in MDCK cells (Maples *et al.*, 1997). In this study, cytochalasin D inhibited basolateral to apical transcytosis, implying the need for a dynamic actin cytoskeleton for transport between early and sorting endocytic compartments (Maples *et al.*, 1997). In contrast, other studies have concluded that apical, but not basolateral, endocytosis involves actin filaments, based on the effects of depolymerizing actin with cytochalasin D (Gottlieb *et al.*, 1993; Jackman *et al.*, 1994; Shurety *et al.*, 1996). This and previous studies have used different epithelial cell types and different endocytic tracers to investigate the role of actin in endocytosis. It is likely that different apical and basolateral pathways of internalization are being measured in different studies. Several other points may account for the differing results obtained with cytochalasin D and JAS on polarized endocytosis. Although JAS and cytochalasin D appear to access filaments through all levels of polarized cells, they might preferentially interact with only some pools of actin and this in turn might depend on the relative stability or lability of actin at the apical or basal cell poles. For instance, actin isoforms have a polarized distribution in gastric parietal cells where β -actin is

found predominantly in the apical region and γ -actin is in the basolateral region (Yao *et al.*, 1995). Regardless of the drugs used, thus, these studies serve to show that actin filaments are involved in endocytosis at both surfaces of polarized epithelial cells.

The effects of JAS-induced polymerization on endocytosis are comparable to those obtained by some manipulations of actin-binding proteins. Myosin I appears to be involved in the distribution of endocytic compartments and in the delivery of ligands to degradative compartments (Durrbach *et al.*, 1996a), in addition to being required for the budding event in receptor-mediated endocytosis in yeast (Geli and Riezman, 1996). The yeast fimbrin homologue, Sac6p, is required for α -factor endocytosis, suggesting that actin filament bundling might facilitate this uptake mechanism (Kubler and Riezman, 1993). The small GTPases Rac and Rho control assembly of the actin cytoskeleton (Hall, 1994; Takai *et al.*, 1995) and their actions influence membrane ruffling, pinocytosis, and various steps of endocytosis. Activated Rac1 and RhoA inhibit receptor-mediated endocytosis and clathrin-coated vesicle formation (Lamaze *et al.*, 1996). Activated RhoA, which causes de novo actin polymerization (Norman *et al.*, 1994), stimulates fluid-phase pinocytosis when microinjected into *Xenopus* oocytes (Schmalzing *et al.*, 1995). More recently, the RhoD protein, which is functionally distinct from other Rho family members, has been localized to the plasma membrane and to early endosomes (Murphy *et al.*, 1996), where it appears to control endosome motility and distribution and homotypic endosome fusion. The effects of various Rho proteins on endocytic pathways and the results of JAS treatment suggest that actin filaments are directly linked to movements of the cell membrane and to endocytic vesicles invaginating from it.

Finally, ultrastructural studies revealed that JAS-induced polymerization created unusual membrane bunches that protrude from the apical cell surface. These bunches were devoid of cytoplasmic organelles, possibly excluded by patches of polymerized actin, but contained all of the microvilli and many associated coated pits. The presence of these bunched membranes may have interfered with endocytosis from the apical cell surface in JAS-treated MDCK cells, although untreated cells had little apical endocytosis in any case. Interestingly, the early endosome marker rab5 gave unusual staining around the periphery of these caps in JAS-treated cells, which might be related to the interaction of rab5 with actin filaments as previously suggested (Murphy *et al.*, 1996). Another unusual ball-like structure containing actin has been observed at the apical surface of 3T3 fibroblasts exposed to a phosphatase inhibitor (Hirano *et al.*, 1992) and this was attributed to effects on actin-myosin-based contractile process. Tension of the contractile ring, a

Figure 12 (facing page). Double labeling of endocytic compartments. JAS-pretreated cells were incubated with FITC-dextran added to the basolateral chamber for 15 or 30 min at 37°C and then stained with primary antibodies followed by Cy3-conjugated antibodies. An antibody against rab5, a marker for early endocytic compartments, did not colocalize with any of the vesicles labeled with FITC-dextran after 15 min uptake (a and b). rab7 (c and d) and M6PR (e and f), markers for late endosomes, showed no colocalization with FITC-dextran after 30 min uptake. TRITC-transferrin showed partial colocalization with labeled compartments in the basal region of the cells but not in the middle region after uptake for 15 min (g and h). Green, FITC-dextran; red, specific antibody or TRITC-transferrin; M, middle region; B, basal region. Bar, 10 μ m.

prominent peripheral band of actin filaments found at the level of the zonulae adherens, is thought to produce the dome-shaped apical surface of yolk sac epithelial cells (King, 1983). Such processes could be analogous to the bunching or purse-string effect we find in JAS-treated cells.

Use of the actin-polymerizing drug JAS on intact cells has provided novel evidence for a role for F-actin in fluid-phase uptake. Our data are consistent with an effect on the initial uptake and later redistribution of endocytosed markers. In particular, JAS induced the clustering but not fusion of perinuclear endosomes. Our data clearly show that F-actin is involved in endocytosis from the basolateral domain in polarized MDCK cells. Alteration of endocytosis in the presence of JAS indicates that a continuous and dynamic assembly and disassembly of actin filaments is normally required for homeostatic regulation of trafficking. Further studies are now required to elucidate the precise mechanism by which F-actin regulates endocytic compartments.

ACKNOWLEDGMENTS

We sincerely thank Drs. Paul Luzio and Rob Parton for their help, discussions, and comments on the manuscript and also Colin MacQueen and Darren Brown for their excellent technical assistance. Antibodies were kindly provided by Drs. Ira Mellman and Chavrier. The Center for Molecular and Cellular Biology is a Special Research Center of the Australian Research Council. J.L.S. is a Wellcome Trust Senior Research Fellow and this work was supported by a National Health and Medical Research Council grant.

REFERENCES

Bomsel, M., Parton, R., Kuznetsov, S.A., Shroer, T.A., and Gruenberg, J. (1990). Microtubule- and motor-dependent fusion in vitro between apical and basolateral endocytic vesicles from MDCK cells. *Cell* 62, 739–731.

Bomsel, M., Prydz, K., Parton, R.G., Gruenberg, J., and Simons, K. (1989). Endocytosis in filter-grown Madin–Darby canine kidney cells. *J. Cell Biol.* 109, 3243–3258.

Brown, D., and Sabolic, I. (1993). Endosomal pathways for water channel and proton pump recycling in kidney epithelial cells. *J. Cell Sci. Suppl.* 17, 49–59.

Brown, D., and Stow, J.L. (1996). Protein trafficking and polarity in kidney epithelium: from cell biology to physiology. *Physiol. Rev.* 76, 245–297.

Bubb, M.R., Senderowicz, A.M.J., Sausville, E.A., Duncan, K.L.K., and Korn, E.D. (1994). Jasplakinolide, a cytotoxic natural product, induces actin polymerization and competitively inhibits the binding of phalloidin to F-actin. *J. Biol. Chem.* 269, 14869–14871.

Crews, P., Manes, L.V., and Boehler, M. (1986). Jasplakinolide, a cyclodepsipeptide from the marine sponge, *Jaspis* sp. *Tetrahedron Lett.* 27, 2797–2800.

de Almeida, J.B., and Stow, J.L. (1991). Disruption of microtubules alters polarity of basement membrane proteoglycan secretion in epithelial cells. *Am. J. Physiol.* 260, C691–C700.

Durrbach, A., Collins, K., Matsudaira, P., Louvard, D., and Coudrier, E. (1996a). Brush border myosin-I truncated in the motor

domain impairs the distribution and the function of endocytic compartments in an hepatoma cell line. *Proc. Natl. Acad. Sci. USA* 93, 7053–7058.

Durrbach, A., Louvard, D., and Coudrier, E. (1996b). Actin filaments facilitate two steps of endocytosis. *J. Cell Sci.* 109, 457–465.

Eker, P., Holm, P.K., van Deurs, B., and Sandvig, K. (1994). Selective regulation of apical endocytosis in polarized Madin–Darby canine kidney cells by mastoparan and cAMP. *J. Biol. Chem.* 269, 18607–18615.

Fath, K.R., and Burgess, D.R. (1993). Golgi-derived vesicles from developing epithelial cells bind actin filaments and possess myosin-I as a cytoplasmically oriented peripheral membrane protein. *J. Cell Biol.* 120, 117–127.

Fuller, S.D., and Simons, K. (1986). Transferrin receptor polarity and recycling accuracy in “tight” and “leaky” strains of Madin–Darby canine kidney cells. *J. Cell Biol.* 103, 1767–1779.

Futter, C.E., Pearse, A., Hewlett, L.J., and Hopkins, C.R. (1996). Multivesicular endosomes containing internalized EGF–EGF receptor complexes mature and then fuse directly with lysosomes. *J. Cell Biol.* 132, 1011–1023.

Geli, M.I., and Riezman, H. (1996). Role of type I myosins in receptor-mediated endocytosis in yeast. *Science* 272, 533–535.

Gottlieb, T.A., Ivanhoe, I.E., Adensnik, M., and Sabatini, D.D. (1993). Actin microfilaments play a critical role in endocytosis at the apical but not the basolateral surface of polarized epithelial cells. *J. Cell Biol.* 120, 695–710.

Gruenberg, J., Griffiths, G., and Howell, K.E. (1989). Characterization of the early endosomes and putative endocytic carrier vesicles in vivo with an assay of vesicle fusion in vitro. *J. Cell Biol.* 108, 1301–1306.

Hays, S.R., Baum, M., and Kokko, J.P. (1987). Effects of protein kinase C activation on sodium, potassium, chloride, and total CO₂ transport in the rabbit cortical collecting tubule. *J. Clin. Invest.* 80, 1561–1570.

Hewlett, L.J., Prescott, A.R., and Watts, C. (1994). The coated pit and macropinocytic pathways serve distinct endosome populations. *J. Cell Biol.* 124, 689–703.

Hirano, K., Chartier, L., Taylor, R.G., Allen, R.E., Fusetani, N., Karaki, H., and Hartshorne, D.J. (1992). Changes in the cytoskeleton of 3T3 fibroblasts induced by the phosphatase inhibitor, calyculin-A. *J. Muscle Res. Cell Motil.* 13, 341–353.

Ikonen, E., de Almeida, J.B., Fath, K.R., Burgess, D.R., Ashman, K., Simons, K., and Stow, J.L. (1997). Myosin II is associated with Golgi membranes: identification of p200 as a nonmuscle myosin II on Golgi-derived vesicles. *J. Cell Sci.* 110, 2155–2164.

Jackman, M.R., Shurety, W., Ellis, J.A., and Luzio, J.P. (1994). Inhibition of apical but not basolateral endocytosis of ricin and folate in Caco-2 cells by cytochalasin D. *J. Cell Sci.* 107, 2547–2556.

Joos, L., and Gicquand, C. (1987). Effect of phalloidin and viroisin on *Acanthamoeba castellanii* after permeabilization. *Biochem. Cell Biol.* 65, 261–270.

King, B.F. (1983). The organization of actin filaments in the brush border of yolk sac epithelial cells. *J. Ultrastruct. Res.* 85, 329–337.

Kreis, T., and Vale, R., Eds. (1993). *Guidebook to the Cytoskeletal and Motor Proteins*. Oxford, United Kingdom: Oxford University Press.

Kubler, E., and Riezman, H. (1993). Actin and fimbrin are required for the internalization step of endocytosis in yeast. *EMBO J.* 12, 2855–2862.

- Lamaze, C., Chuang, T.-H., Terlecky, L.J., Bokoch, G.M., and Schmid, S.L. (1996). Regulation of receptor-mediated endocytosis by Rho and Rac. *Nature* 382, 177–179.
- MacLean-Fletcher, S., and Pollard, T.D. (1980). Mechanism of action of cytochalasin B on actin. *Cell* 20, 329–341.
- Maples, C.J., Ruiz, W.G., and Apodaca, G. (1997). Both microtubules and actin filaments are required for efficient postendocytotic traffic of the polymeric immunoglobulin receptor in polarized Madin-Darby canine kidney cells. *J. Biol. Chem.* 272, 6741–6751.
- Matteoni, R., and Kreis, T.E. (1987). Translocation and clustering of endosomes and lysosomes depends on microtubules. *J. Cell Biol.* 105, 1253–1265.
- Mayor, S., Presley, J.F., and Maxfield, F.R. (1993). Sorting of membrane components from endosomes and subsequent recycling to the cell surface occurs by a bulk flow process. *J. Cell Biol.* 121, 1257–1269.
- Muallem, S., Kwiatkowska, K., Xu, X., and Yin, H.L. (1995). Actin filament disassembly is a sufficient trigger for exocytosis in non-excitable cells. *J. Cell Biol.* 128, 589–598.
- Murphy, C., Saffrich, R., Grummt, M., Gournier, H., Rybin, V., Rubino, M., Auvinen, P., Lutcke, A., Parton, R.G., and Zerial, M. (1996). Endosome dynamics regulated by a Rho protein. *Nature* 384, 427–432.
- Narula, N., McMorrow, I., Plopper, G., Doherty, J., Matlin, K.S., Burke, B., and Stow, J.L. (1992). Identification of a 200-kD, Brefeldin-sensitive protein on Golgi membranes. *J. Cell Biol.* 117, 27–38.
- Norman, J.C., Price, L.S., Ridley, A.J., Hall, A., and Koffer, A. (1994). Actin filament organization in activated mast cells is regulated by heterotrimeric and small GTP-binding proteins. *J. Cell Biol.* 126, 1005–1015.
- Parton, R.G., Prydz, K., Bomsel, M., Simons, K., and Griffiths, G. (1989). Meeting of the apical and basolateral endocytic pathways of the Madin-Darby canine kidney cell in late endosomes. *J. Cell Biol.* 109, 3259–3272.
- Reizman, H. (1993). Yeast endocytosis. *Trends Cell Biol.* 3, 273–277.
- Ridley, A.J. (1996). RHO-themes and variations. *Current Biol.* 6, 1256–1264.
- Robinson, L.J., Pang, S., Harris, D.S., Heuser, J., and James, D.E. (1992). Translocation of the glucose transporter (GLUT4) to the cell surface in permeabilized 3T3-L1 adipocytes: effects of ATP, insulin, and GTP γ S and localization of GLUT4 to clathrin lattices. *J. Cell Biol.* 117, 1182–1196.
- Rodriguez-Boulan, E., and Nelson J. (1989). Morphogenesis of the polarized epithelial cell phenotype. *Science* 245, 718–725.
- Sandvig, K., and van Deurs, B. (1990). Selective modulation of the endocytic uptake of ricin and fluid phase markers without alteration of transferrin endocytosis. *J. Biol. Chem.* 265, 6382–6388.
- Schmalzing, G., Richter, H.P., Hansen, A., Schwarz, W., Just, I., and Aktories, K. (1995). Involvement of the GTP binding protein Rho in constitutive endocytosis in *Xenopus laevis* oocytes. *J. Cell Biol.* 130, 1319–1332.
- Senderowicz, A.M.J., Kaur, G., Sainz, E., Laing, C., Inman, W.D., Rodriguez, J., Crews, P., Malspeis, L., Grever, M.R., Sausville, E.A., and Duncan, K.L. K. (1995). Jaspakinolide's inhibition of the growth of prostate carcinoma cells in vitro with disruption of the actin cytoskeleton. *J. Natl. Cancer Inst.* 87, 46–51.
- Shurety, W., Bright, N.A., and Luzio, J.P. (1996). The effects of cytochalasin D and phorbol myristate acetate on the apical endocytosis of ricin in polarised Caco-2 cells. *J. Cell Sci.* 109, 2927–2935.
- Stossel, T.P., Chaponnier, C., Ezzel, R.M., Hartwig, J.H., Janmey, P.A., Kwiatkowski, D.J., Lind, S.E., Smith, D.B., Southwick, F.S., Yin, H.L., and Zaner, K.S. (1985). Non-muscle actin binding proteins. *Annu. Rev. Cell Biol.* 1, 353–402.
- Takai, Y., Sasaki, T., Tanake, K., and Nakanishi, H. (1995). Rho as a regulator of the cytoskeleton. *Trends Biochem. Sci.* 20, 227–231.
- Tapon, N., and Hall, A. (1997). Rho, Rac, and Cdc42 GTPases regulate the organization of the actin cytoskeleton. *Curr. Opin. Cell Biol.* 9, 86–92.
- Thilo, L., Stroud, E., and Haylett, T. (1995). Maturation of early endosomes and vesicular traffic to lysosomes in relation to membrane recycling. *J. Cell Sci.* 108, 1791–1803.
- van Deurs, B., Holm, P.K., Kayser, L., and Sandvig, K. (1995). Delivery to lysosomes in human carcinoma cell line HEP-2 involves an actin filament-facilitated fusion between mature endosomes and preexisting lysosomes. *Eur. J. Cell Biol.* 66, 309–323.
- von-Bonsdorff, C.H., Fuller, S.D., and Simons, K. (1985). Apical and basolateral endocytosis in Madin-Darby canine kidney (MDCK) cells grown on nitrocellulose filters. *EMBO J.* 4, 2781–2792.
- Wehland, J., Osborn, M., and Weber, K. (1980). Phalloidin associates with microfilaments after microinjection into tissue culture cells. *Eur. J. Cell Biol.* 21, 188–194.
- Weibel, E.R. (1980). *Stereological Methods*. New York: Academic Press.
- Yao, X., Chaponnier, C., Gabbiani, G., and Forte, J.G. (1995). Polarized distribution of actin isoforms in gastric parietal cells. *Mol. Biol. Cell* 6, 541–557.
- Zabriskie, T.M., Klocke, J.A., Ireland, C.M., Marcus, A.H., Molinski, T.F., Faulkner, D.J., Xu, C., and Clardy, J.C. (1986). Jaspamide, a modified peptide from a Jaspis sponge, with insecticidal and antifungal activity. *J. Am. Chem. Soc.* 108, 3123–3124.